0026-895X/02/6101-150–159$3.00
MOLECULAR PHARMACOLOGY
Copyright © 2002 The American Society for Pharmacology and Experimental Therapeutics
Mol Pharmacol 61:150–159, 2002

Vol. 61, No. 1
1134/951373
Printed in U.S.A.

A Novel Human Nicotinic Receptor Subunit, α10, That Confers Functionality to the α9-Subunit

FRÉDÉRIC SGARD, ERIC CHARPANTIER, SONIA BERTRAND, NANCY WALKER, DANIEL CAPUT, DAVID GRAHAM, DANIEL BERTRAND, and FRANÇOIS BESNARD

Sanofi-Synthélabo, Department of Molecular and Functional Genomics, Rueil-Malmaison, France (F.S., E.C., N.W., D.C., D.G., F.B.); and Department of Physiology, Centre Médical Universitaire, Geneva, Switzerland (E.C., S.B., D.B.)

Received June 1, 2001; accepted September 21, 2001

This paper is available online at http://molpharm.aspetjournals.org

ABSTRACT

We present herein the cloning of the human nicotinic acetylcholine receptor α9-ortholog and the identification of a new α-like subunit (α10) that shares 58% identity with α9. Whereas α10 fails to produce functional receptors alone, it promoted robust acetylcholine-evoked currents when coinjected with α9. The presence of α10 modifies the physiological and pharmacological properties of the α9 receptor indicating that the two subunits coassemble in a single functional receptor. Fusing the N-terminal domain of α9 with the rest of the α10-cDNA yielded a functional α9:α10-chimera that displays the acetylcholine binding properties of α9 and ionic pore characteristics of α10-containing receptors. In addition, α9- and α10-subunit mRNAs show limited similar tissue distribution patterns and are expressed in cochlea, pituitary gland, and keratinocytes. These data suggest that, in vivo, α9-containing receptors coassemble with α10-subunit.

Nicotinic acetylcholine receptors are members of the ligand-gated ion channel superfamily that are formed by the pentameric association of multiple subunits (Galzi and Changeux, 1995). In vertebrates, neuronal nAChR subunits are encoded by a large family of genes and many of them have already been identified in humans (Boyd, 1997). Special interest has been devoted to the α7- to α9-subunits that have the unique capacity of forming functional homomeric receptors (Couturier et al., 1990; Anand et al., 1993; Elgoyhen et al., 1994; Gotti et al., 1994). Expression of the most recently cloned subunit in this subfamily, α9, has been described in only very restricted areas such as the pituitary pars tuberalis, the olfactory epithelium and in the cochlea (Elgoyhen et al., 1994). In particular, this subunit has been shown to be expressed on the cochlear outer hair cells (OHCs), where it is supposed to mediate the cholinergic efferent transmission (Puel, 1995), which activates hyperpolarizing current mediated by small conductance calcium-activated potassium channels (Oliver et al., 2000). Functional properties of the receptors obtained by expression of the α9-subunit closely resemble those of native nAChRs from OHC that display very original pharmacological features (Erostegui et al., 1994; Guth and Norris, 1996). However, the amplitude of the acetylcholine-evoked currents generated by the expression of the α9-subunit in *Xenopus laevis* oocyte remains unusually small and the fraction of positive cells very low. These data suggest that although able to reconstitute homomeric receptors, the α9-subunit may require another subunit to be fully functional, although attempts to coexpress α9 with other known α nAChR subunits failed to generate functional receptors (Elgoyhen et al., 1994). Because other genes coding for neuronal nAChRs could well exist in the human genome, we have sought to clone the human α9-subunit and examined the possibility of identifying the missing α9-partner.

Materials and Methods

Cloning of the Human α9- and α10-cDNAs. The rat α9-nAChR amino acid sequence (Swissprot accession number P43144) was used to perform a TblastN search against an expressed sequence tag (EST) database. A single EST was identified which presented a high degree of homology with the rat α9-sequence and the corresponding cDNA clone originating from a human whole embryo (8-week-old) cDNA library was retrieved. This cDNA clone was found to contain a nearly complete open reading frame (ORF) coding for the human α9 nAChR subunit. An unspliced intron was present which was removed by PCR. The sequence corresponding to the missing 5′ end of the ORF and a portion of the 5′-untranslated region was obtained from human genomic DNA using the Genome Walker system (CLONTECH, Palo Alto, CA). An oligonucleotide containing 16 nucleotides of the 5′-untranslated region and the first 18 nucleotides of the ORF was then synthesized to complete the original cDNA by

This work was supported in part by a Swiss National Science Foundation grant (to D.B.).

ABBREVIATIONS: nAChR, nicotinic acetylcholine receptor; EST, expressed sequence tag; OHC, outer hair cells; ORF, open reading frame; bp, base pair(s); PCR, polymerase chain reaction; RACE, rapid amplification of cDNA ends; RT, reverse transcription; ACh, acetylcholine; α-bgt, α-bungarotoxin; BAPTA-AM, 1,2-bis(2-aminophenoxy)ethane-*N*′,*N*,*N*′,*N*′-tetraacetic acid-acetoxymethyl ester.

PCR. The resulting full-length cDNA clone (GenBank accession number AJ243342) was sequenced and inserted into the pTracer-EF eukaryotic expression vector (Invitrogen, Carlsbad, CA) for further use.

The TblastN search also resulted in the identification of an EST from the GenBank database (accession number AA243627) that had been identified as a putative homolog of the rat α9-subunit but whose sequence identity was lower than that expected for the α9-ortholog. The clone was obtained from the IMAGE Consortium (685357; http://image.llnl.gov/) and its sequencing showed that it contained a partial ORF corresponding to a novel nAChR α-subunit. A 700-bp fragment of the α10-cDNA was used as a probe to analyze α10-mRNA expression in human tissues to obtain the missing coding sequence. Strong hybridization was observed in skeletal muscle and human Marathon (CLONTECH) skeletal muscle cDNA was used to clone the 5′ coding region of the α10-cDNA by 5′ RACE. Those experiments showed the presence of two unspliced introns in this 5′ region. Total coding sequence (GenBank accession number AJ278118) was obtained from several RACE-PCR products and a full-length cDNA clone containing the entire coding sequence was then obtained by RT-PCR from human pituitary mRNA and inserted in pTracer-EF vector. Detailed intron-exon boundaries were analyzed by sequencing PCR products obtained from human genomic DNA.

Chromosomal Localization of α10-Gene. A PAC containing the sequence of α10 was isolated by PCR using oligonucleotide primers flanking an intron. It was then used to localize the α10 gene to 11p15.5 using fluorescence in situ hybridization (Incyte Genomics, Palo Alto, CA).

Northern Blot Analysis. Multiple human tissue Northern blots (2 μg/lane; CLONTECH) were hybridized with a *Bsp*HI 360-bp fragment of the α10-cDNA. The probe was radiolabeled with [^{32}P]dCTP (PerkinElmer Life Sciences, Boston, MA) using the random priming technique (Megaprime labeling kit; Amersham Biosciences, Little Chalfont, Buckinghamshire, UK). Stringent washing conditions (65°C; 0.1× standard saline citrate/0.1% SDS) were used. The blots were scanned using an STORM 860 Imager (Molecular Dynamics, Sunnyvale, CA).

Analysis of α9- and α10-mRNA Expression by RT-PCR. Human pituitary gland mRNA was obtained from CLONTECH. Rat total RNA from pituitary gland, tongue, nasal epithelium, and cochlea was isolated from frozen tissues dissected from adult Sprague-Dawley rats using RNeasy silica-gel membrane spin columns (QIAGEN, Hilden, Germany). First strand cDNA synthesis was carried out using 50 ng of mRNA or about 1 μg of total RNA with the SuperScript reverse transcriptase (Invitrogen). Specific human and mouse α9- and α10- and rat α10-primers were designed for PCR amplification: human α9, ctacaatggcaatcaggtgg and atgatggtcaacgcagtgg (predicted amplified fragment length, 425 bp); human α10, tctcaagctgttccgtgacc and aaggctgctacatccacgc (predicted amplified fragment length, 391 bp); mouse α9, ccttacccagatgtcaccttcactc and aacaccatagcaaagaaaatccaca (predicted amplified fragment length, 177 bp); mouse α10, aatgtgaccctggaggtgac and gtaggcatctgtccacacytg (predicted amplified fragment length, 108 bp); and rat α10, tgagaccagtggcagatacag and ccattcaacgttctccacg (predicted amplified fragment length, 472 bp). The predicted amplified fragments contain either one or two intron positions, those in α10-segments being known to correspond to unspliced introns in human skeletal muscle. PCRs were performed on 5 μl of the 20 μl of cDNA synthesis volume using the Expand long template polymerase mix (Roche Diagnostics, Mannheim, Germany) and buffer, 0.5 mM dNTP, 0.5 μM each primer in the following cycling conditions: 3 min at 94°C followed by 35 cycles of 30 s at 94°C, 30 s at 58°C (rat α10 primers) or 64°C (human α9 and α10 primers), and 1 min at 68°C, followed by 5 to 10 cycles of 30 s at 94°C, 30 s at 58 or 64°C, and 1 min at 68°C with an auto-extension step of 20 s per cycle, followed by 4 min at 68°C. All PCR products were subcloned into pCR-II Topo (Invitrogen) vector and sequenced.

Full-length α10-cDNA containing the entire open reading frame used for expression analysis was obtained using the following primers: tcacatccagagacctgcc and tgagagctccaatacccagc. PCR conditions were as described above with the following cycling conditions; 3 min at 94°C followed by 25 cycles of 30 s at 94°C, 30 s at 61°C, and 1.5 min at 68°C, followed by 10 cycles of 30 s at 94°C, 30 s at 58 or 64°C, and 1.5 min at 68°C with an autoextension step of 10 s per cycle, followed by 4 min at 68°C.

Western Blot Experiments. Human epidermal keratinocytes were obtained from BioWhittaker Inc. (Walkersville, MD) and grown as recommended by the supplier. COS cells were transfected using FuGene (Roche Diagnostics) according to the manufacturer's instructions using 2 μg of vector. Protein extracts were obtained by recovering cell monolayers in lysate buffer [100 μl of Laemmli buffer (Bio-Rad, Hercules, CA)/5% (v/v) β-mercaptoethanol and 50 μl of PBS were used for 4×10^5 cells]. Twenty microliters of cell lysate per lane was loaded onto SDS-polyacrylamide gel electrophoresis 4 to 15% gradient acrylamide gel (Bio-Rad) and proteins separated by electrophoresis. The gels were electroblotted onto a nitrocellulose membrane (Amersham Biosciecnes). The membranes were blocked with 5% nonfat milk/0.1% Tween 20 (Sigma, St Louis, MO) in PBS buffer for 1 h. Each membrane was incubated with a primary anti-α10 antibody (Eurogentech, Seraing, Belgium) diluted to 10 μg/ml in PBS supplemented with 0.1% Tween 20, 5% nonfat milk, washed three times in PBS-Tween 20 0.1%, and incubated 1 h with a secondary goat anti-rabbit antibody conjugated to horseradish peroxidase (Sigma) diluted 1:10,000. Binding was visualized with the ECL Western blot detection system (Amersham Biosciecnes).

For control experiments in which the specificity of binding was tested, the primary anti-α10 serum was preincubated for 1 h with 200 μg/ml of the immunizing peptide (CGQSRPPELSPSPQSPE) in PBS-0.5% Tween 20.

In Situ Hybridization. RT-PCR was used to amplify a 494-base pair cDNA (corresponding to nucleotide 180–674 of the GenBank sequence AF196344) from rat pituitary mRNA. The T7 promoter was added by a second PCR and then the cDNA was purified after gel electrophoresis and sequenced. The riboprobe was transcribed with ^{35}S-labeled UTP, purified by phenol/chloroform extraction, and precipitated.

Brains from Sprague-Dawley male rats (180–200 g) and E18 rat embryos were frozen. Fifteen-micrometer-thick cryostat sections were defrosted, rehydrated, and fixed with 4% paraformaldehyde. After proteinase K treatment, acetylation, and prehybridization, the slides were hybridized overnight at 55°C with 5×10^4 cpm/μl of probe in a hybridization solution (60% formamide, 300 mM NaCl, 20 mM Tris, pH 7.4, 5 mM EDTA, pH 8, 10% dextran sulfate, 0.4 ng/μl tRNA, 1× Denhardt's solution, and 200 mM dithiothreitol). After high stringency washes, slides were dehydrated and dipped in Kodak NBT2 emulsion and stored for 1 month in the dark at 4°C. After development the slides were lightly colored with Hemalun, mounted, and examined with light- and dark-phase microscopy.

Oocyte Preparation and Injection. *X. laevis* oocytes were isolated and prepared as described previously (Bertrand et al., 1991). The oocytes were intranuclearly injected with 2 ng of expression vector cDNA. They were kept in a separate well of a 96-well microtiter plate at 18°C. OR2 control medium consisted of 88 mM NaCl, 2.5 mM KCl, 10 mM HEPES, 1 mM $MgCl_2$, and 2 mM $CaCl_2$, pH 7.4, adjusted with NaOH.

Electrophysiology. Throughout each experiment, oocytes were continuously superfused with control medium and fluid exchanges were controlled by electromagnetic valves. Gravity-feed solution was flowing at an approximate rate of 6 ml/min. Oocytes were measured 2 to 4 days after cDNA injections. Electrophysiological recordings were performed using a two-electrode voltage-clamp (GeneClamp amplifier; Axon Instruments, Union City, CA). Electrodes were made of borosilicate glass, pulled with a BB-CH-PC puller (Mecanex, Nyon, Switzerland), and filled with a filtered 3 M KCl. Unless specified, the holding potential was −75 mV. Oocytes were continuously maintained at 18°C during preparation and experiments. Calcium

permeability measurements were effectuated using *N*-methyl-D-glucamine and oocytes were incubated for at least 6 h with the calcium chelator 1,2-bis(2-aminophenoxy)ethane-*N*′,*N*,*N*′,*N*′-tetraacetic acid-acetoxymethyl ester (BAPTA-AM) to prevent activation of the endogenously expressed calcium activated chloride currents (Boton et al., 1989). Data from the reversal potential were fitted using a Hodgkin-Goldman-Katz constant field equation appropriately adapted (Jagger et al., 2000; Katz et al., 2000). Calcium blockade was simulated using the empirical Hill equation (see Katz et al., 2000).

Binding Experiments. Measure of receptor expression on the oocyte surface was carried out using ^{125}I-α-bgt (2000 Ci/mmol, Amersham). Oocytes were incubated for 2 h in 200 μl of a 50 nM solution of ^{125}I-α-bgt in OR2 buffer and briefly washed four times with OR2, and the amount of radioactivity determined by γ-counting. Electrophysiological recordings were carried out to verify proper expression of α9- or α9-α10-expression.

Results

Cloning of the Human α9-Subunit. A search by homology was performed against human EST databases using the rat α9 nAChR amino acid sequence. A single EST was found with very high homology and the relevant cDNA clone was fully sequenced. The results showed that this clone encoded a protein displaying more than 90% identity to the rat α9 sequence. A full-length cDNA clone was then constructed and inserted into an expression vector (see *Materials and Methods*).

The resulting clone encodes a 479-amino acid polypeptide with a predicted molecular mass of 54.7 kDa. The human α9-deduced amino acid sequence exhibits 90.8% identity with its rat homolog (Fig. 1A).

Identification and Isolation of a Novel Human nAChR α-Subunit. The homology search carried out in the human databases with the rat α9-nAChR amino acid sequence also identified a different EST that showed relatively high homology to the α9-subunit sequence. The missing 5′ extremity of the corresponding partial cDNA clone was then obtained by 5′ RACE and a continuous cDNA containing the entire open reading frame was generated by RT-PCR from human pituitary mRNA. This ORF encoded for a 450-amino acid polypeptide (Fig. 1A) and classified as the nAChR α10-subunit. Amino acid comparison with the other known nAChR subunit (Fig. 1B) indicates that this novel α10-subunit is more closely related to the subunits that are able to form functional homomeric receptors (α7, α8, and α9) rather than to those requiring a β-subunit for functional expression.

Using fluorescence in situ hybridization to human chromosomes, the α10 gene was mapped to 11p15.5. This region contains a number of genetic diseases loci and most noticeably a locus linked to a deficit in inhibitory gating phenotype related to the brain's response to auditory stimuli (Freedman et al., 1994), although more precise genetic mapping would be required to link α10 to this locus.

Analysis of α10-Expression. Because α10 presents relatively high amino acid sequence similarity with α9, mRNA expression of α10 was investigated in tissues known to express the α9-subunit. The presence of both α9- and α10-transcripts was detected by RT-PCR in human pituitary gland (Fig. 2A) from which a cDNA encoding the complete coding sequence was isolated and in keratinocytes (not shown). In addition, the presence of partially spliced α10-transcript was also detected in these tissues. Northern blot analysis showed a strong expression of a single 6.4-kilobase transcript in skeletal muscle and a faint signal in heart (not shown). However, RT-PCR experiments showed that this transcript is not completely spliced in these tissues, and as such would not be translated into a full-length α10-protein. Further analysis showed that the position of introns within the gene structure (Fig. 1A) is similar to that described for the rat α9-gene (Elgoyhen et al., 1994).

To verify that correctly processed α10-mRNA leads to the expression of α10-protein, a Western blot analysis was carried out on human keratinocyte protein extract. The results (Fig. 2B) show that an affinity-purified anti-α10 antibody recognized a major protein band of about 55 kDa. The specificity of the antibody was confirmed in control experiments showing that the staining of this band could be eliminated by preincubating the antibody solution with the α10-peptide

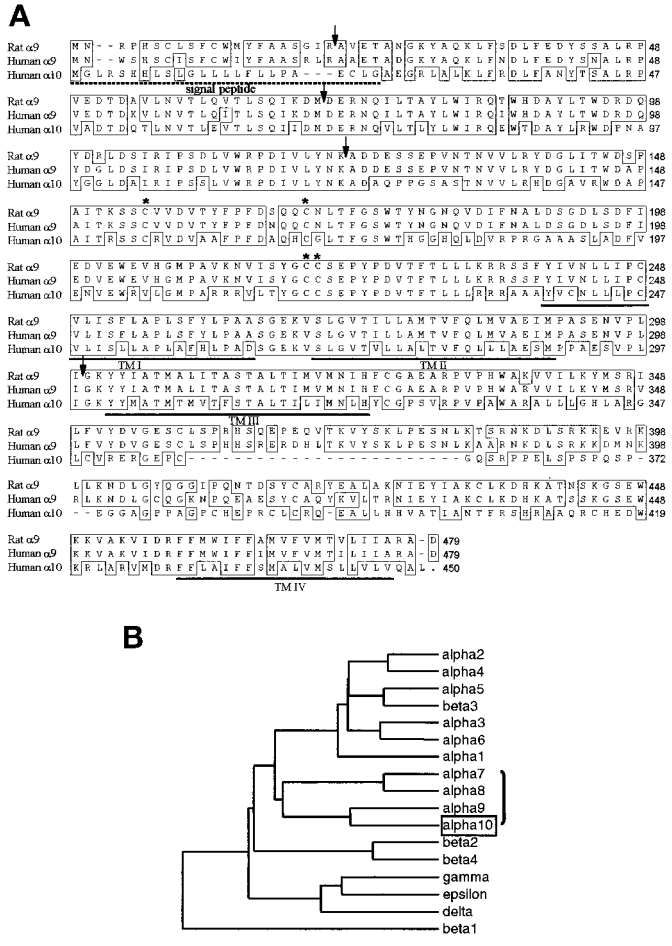

Fig. 1. Comparison of the deduced amino acid sequences from the human α9- and α10-subunits together with sequences of other nAChR subunits. A, alignment of the deduced human α9- and α10-subunit with the rat α9-subunit. Identical residues between the three subunit sequences are boxed. The predicted signal peptides are underlined in dotted line while predicted transmembrane domains (TM) are underlined in bold line. *, characteristic cysteine residues found in all nAChR α-subunits. Arrows indicate the positions of the four introns detected within the coding sequences of both α9- and α10-genes. B, dendrogram illustrating the relationship between the novel α10-subunit (boxed) and the other known nAChR subunits. This tree was generated from the alignment (Clustal W software) of all known human nAChR subunit amino acid sequences together with the chick α8-subunit. Square bracket highlights the closer similarity between α10 and the other subunits known to form functional homo-oligomeric receptors.

used for immunization and that a band of similar size could be labeled with protein extract from α10-transfected but not from α9-transfected COS cells (Fig. 2B).

RT-PCR analysis was also carried out on rat for tissues that were not available from human, the rat α10 ortholog sequence having recently been deposited in GenBank (accession number AF196344). A PCR product corresponding to α10-mRNA with properly spliced introns 2 and 3 was also detected in the rat pituitary gland and in the cochlea, although, in contrast, no α10- signal was detected in rat tongue or whole brain (Fig. 2A). Similarly, both α9- and α10-transcripts were found (not shown) in the UB/OC-2 mouse cochlear cell line known to express α9-containing nAChRs (Jagger et al., 2000). A cRNA rat α10-probe was also hybridized onto sections of adult rat brain. α10-mRNA expression was found in the pars tuberalis region of the pituitary gland (Fig. 3), exactly as described previously for the rat α9-transcript (Elgoyhen et al., 1994).

Functional Expression of α9 and α10 in *X. laevis* Oocytes. Reconstitution experiments of the human α9- and α10-subunits were carried out by intranuclear cDNA injections in *X. laevis* oocytes. Expression of the human α9-cDNA yielded functional receptors that can be activated by acetylcholine with an EC_{50} of 30 ± 6 μM (Fig. 4A; Table 1). However, the amplitude of this acetylcholine-evoked current was small by comparison with current recorded in sibling oocytes expressing the homomeric human α7 receptor (not shown). The human α9-receptor also exhibited a peculiar pharmacological profile similar to that displayed by the rat ortholog. For example, nicotine evoked no detectable currents but acted as an antagonist with an IC_{50} of 41.2 ± 5.4 μM (not shown).

Surprisingly, despite its homology with α9, α10-cDNA failed to reconstitute functional homomeric receptors in *X. laevis* oocytes. Application of acetylcholine concentrations up to 1 mM elicited no currents in cells injected with this sub-

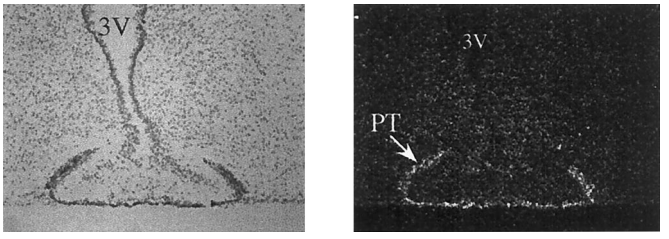

Fig. 3. In situ hybridization of α10-mRNA in rat pituitary. Bright (A) and dark (B) field pair photomicrographs of adult rat brain section through the third ventricule (3V) hybridized with α10-cRNA. Hybridization is apparent in the pars tuberalis (PT) of the pituitary.

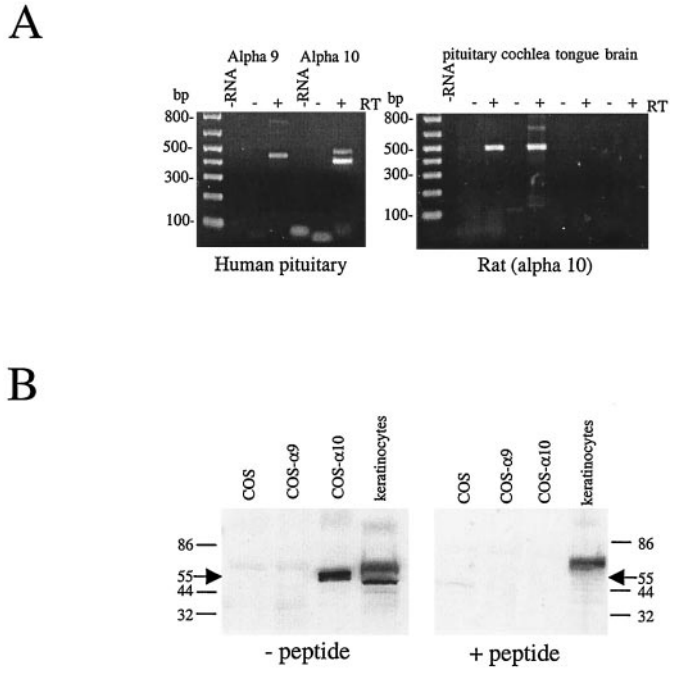

Fig. 2. Analysis of α9- and α10-expression by RT-PCR (A) and western blot (B). A, RT-PCR results obtained from human and rat tissue RNAs using α9- and α10-specific primers. A sample of 5 μl of each reaction was loaded on ethidium bromide-stained agarose gels. The two α10-fragments seen for human pituitary correspond to fully spliced transcript (391 bp) and transcript with a partially spliced intron 2 (453 bp). B, visualization of α10-subunit expression in human keratinocytes by western blot. A 55-kDa band is specifically recognized. A band of slightly higher molecular mass (about 58 kDa, possibly due to different glycosylation) is recognized for α10-transfected COS cells. Preincubation of the anti-α10 antibody with 200 nmol of immunizing peptide abolishes the detection of the protein. No staining was detected for COS or α9-transfected COS cell protein extracts.

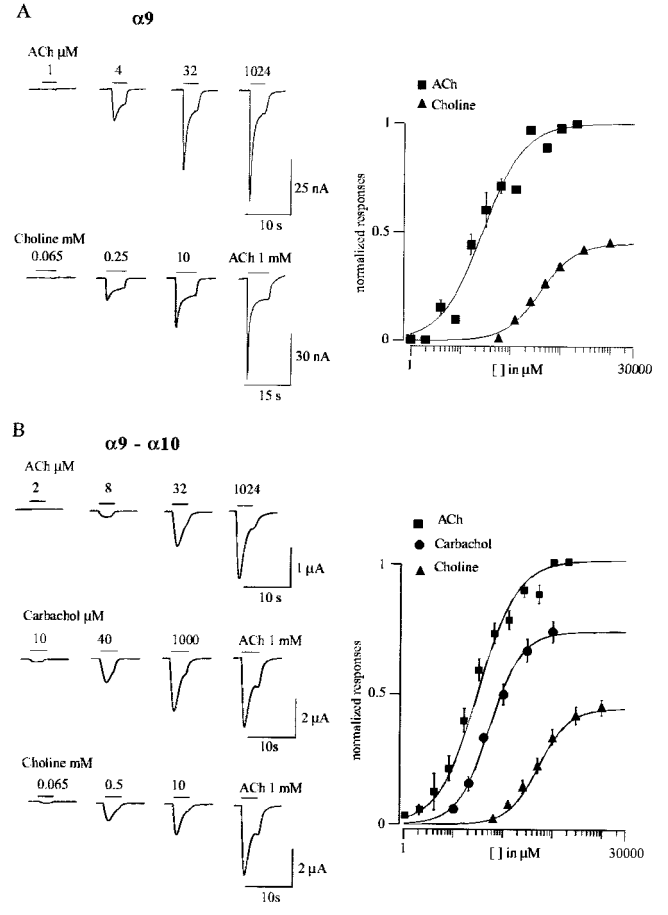

Fig. 4. Properties of α9- and α9-α10-expressing oocytes. A, acetylcholine and choline evoked currents in oocytes expressing the human α9-receptor. Left illustrates typical currents evoked by three concentrations of these two agonists. Concentration-response curves to acetylcholine and choline are represented in the right. B, oocytes expressing the α9- and α10-subunits display robust currents in response to acetylcholine, carbachol or choline. Typical currents are presented in the left and concentration-response relationships in the right. Lines through the data points are best fit obtained with the Hill equation. Corresponding values are given in Table 1.

unit alone (not shown). Coinjection of the available β-subunits (β2 and β4) remained ineffective, and no current could be detected in any of the configurations tested (not shown). In contrast, robust ACh-evoked currents were recorded in oocytes injected with equivalent amounts of both the α9- and α10-cDNAs (Fig. 4B). Comparison of the amplitudes of the ACh-evoked currents in oocytes injected with the α9-α10 mixture or α9 alone confirmed that presence of the α10-subunit markedly influences the amplitude of the acetylcholine evoked currents, suggesting that this protein is probably integrated in the α9-receptor complexes.

To examine further this phenomenon, the physiological and pharmacological profiles of receptors reconstituted in oocytes injected with the α9-α10 mixture or α9 alone were compared. Although it is known that acetylcholine is the natural agonist of α9-containing receptors and that these receptors are inhibited by nicotine (Elgoyhen et al., 1994), little information is available regarding other agonists. Choline in the millimolar range is a powerful agonist of the homomeric α7-receptors (Papke et al., 1996). As shown in Fig. 4A, choline behaves as a partial agonist at α9-expressing oocytes with an EC_{50} in the high micromolar range (Table 1). Comparison of the concentration-response curves evoked by either acetylcholine or choline reveals no significant differences between oocytes injected with α9 alone or the α9-α10 mixture (Fig. 4). Concentration-response curves obtained with carbachol illustrate that this substance also acts as a partial agonist that evokes about 76% ± 4 (n = 6; Table 1) of the maximal acetylcholine-evoked current in oocytes injected with the α9-α10 mixture. No differences in response time-courses could be observed between α9 and α9-α10 expressing oocytes for the agonists tested. Other typical nicotinic receptor agonists such as epibatidine or 1,1-dimethyl-4-phenylpiperazinium only elicited very small responses on α9-α10 expressing oocytes (Table 1). Moreover, as predicted on the basis of the α9 properties, nicotine acted as an antagonist at the α9-α10 receptor (not shown).

As complementary characterization, we then examined the effects of competitive and noncompetitive inhibitors. It has been widely documented that the snake toxin α-bgt is a potent competitive inhibitor of homomeric α7- and α9-receptors (Couturier et al., 1990; Elgoyhen et al., 1994). Although this toxin blocks in a quasi-irreversible manner homomeric chick α7 nAChRs (Couturier et al., 1990), reversibility has been described on nicotinic receptors from guinea pig OHC (Lawoko et al., 1995). In agreement with these previous observations, exposures to α-bgt (100 nM, 30 min) caused almost a complete inhibition of the acetylcholine-evoked current (Fig. 5A, upper). Reversibility of this blockade was, however, observed within 15 to 40 min after the toxin had been removed. Homomeric α9 receptors displayed an IC_{50} to α-bgt of about 2.1 nM (n = 5), whereas half -blockade was observed only at 14 nM (mean of two to six cells for each data point) in oocytes expressing α9-α10 (Fig. 5B). The 7-fold difference in sensitivity to α-bgt suggests that α10 must participate in the formation of the receptor binding site and therefore that both α9 and α10 can assemble in the same receptor complex. Challenge with the antagonist d-tubocurarine revealed that this compound inhibits the homomeric α9 receptors with an IC_{50} of roughly 2 μM, whereas half-inhibition of α9-α10-expressing oocytes was already observed at 0.73 μM (Figs. 5, C and D). Both the low Hill coefficient and the increase in the response decay caused by d-tubocurarine on α9-α10-expressing oocytes suggest that this compound may act as an open channel blocker at this receptor subtype. The higher Hill coefficient of d-tubocurarine concentration-response curve at α9-receptors indicates that this compound may preponderantly act as a competitive inhibitor at the homomeric form of this receptor. In addition, the lower IC_{50} value of these receptors for d-tubocurarine indicates an interaction with different amino acid residues.

Whether the difference between current amplitude obtained with α9 alone or α9-α10-subunits was due to either a low level of α9-surface expression or the fact that functional receptors require the assembly of the two subunits was analyzed by measuring α-bgt binding on oocyte surface. Interestingly, a significant amount of α-bgt binding was observed in oocytes injected with the α9-subunit alone (Table 2). Significant amount of α-bgt binding was also observed in α9-α10 oocytes but for technical difficulties, no attempt was made to correlate the current amplitude and amount of binding.

One of the common biophysical properties of all the neuronal nicotinic acetylcholine receptors is their strong inward rectification (Couturier et al., 1990; Mathie et al., 1990; Elgoyhen et al., 1994). Highly nonlinear current-voltage (I-V) relationships were also reported for the α9-receptor (Katz et al., 2000), indicating that these receptors may be more complex than more classical nAChRs. A typical rectification was observed when voltage ramps protocols were performed from positive to negative, whereas an outward rectification was

TABLE 1

Comparison of responses of α9 and α9-α10 expressing oocytes to different nicotinic ligands. Values are indicated with their respective S.E.M. The number of cells tested in each condition is indicated in parenthesis.

Agonists	α9–α10			α9		
	ACh Response	EC_{50}	n_H	ACh Response	EC_{50}	n_H
	%	μM		%	μM	
ACh		27 ± 6 (8)	1.05 ± 0.04		30 ± 6 (10)	1.1 ± 0.08
Carbachol (1 mM*)	76 ± 4 (6)	57 ± 2 (4)	1.35 ± 0.1			
Choline (10 mM*)	57 ± 4 (8)	519 ± 41 (3)	1.4 ± 0.1	45 ± 2 (4)	400 ± 23 (4)	1.2 ± 0.1
Suberyldicholine (1 mM*)	39 ± 4 (3)					
DMPP (100 μM*)	7 ± 4 (4)					
ATP (1 mM*)	3 ± 2 (4)					
(±)-Epibatidine (10 μM*)	0.14 ± 0.07 (4)					
Cytisine (100 μM*)	0 (4)					
(−)-Nicotine (100 μM*)	0 (4)			0 (4)		

* Concentration used to determine % of ACh response.
n_H, Hill coefficient.

observed when the ramp was effectuated in the opposite direction (Fig. 6A). The comparable inward rectification observed with different steady holding current (Fig. 6B) suggests that the difference between positive to negative ramp is attributable to a slowly appearing channel blockade. Because of the time persistence of this blockade, negative to positive ramps failed to relieve the block, and only the outward rectification is observed. Thus, coexpression of the α10-subunit causes no detectable modification of the receptor I-V curve. Because a negative reversal potential was observed both in BAPTA-AM treated cells and in absence of extracellular calcium (data not shown), it must be attributed to a permeability ratio of sodium versus potassium slightly lower than unity (best fit was obtained with a pNa/pK of 0.65).

Chimeric α9-α10-Subunits Form Fully Functional Acetylcholine Receptors. Considering the relatively high homology between α9- and α10-amino acid sequences, it was surprising to find that homomeric α10-receptors could not form functional ligand-gated channels. To get a better understanding of the structural features behind this difference we constructed and analyzed the properties of a chimeric α9:α10-subunit. The chimeric α9:α10-cDNA was obtained by fusing the amino-terminal region of α9 up to the first predicted membrane-spanning domain with from this point the remaining 3′ sequence coding for the α10-subunit (Fig. 7A). The resulting construct was injected into *X. laevis* oocytes and the electrophysiological responses to acetylcholine analyzed. As shown in Fig. 7B, robust currents were evoked in

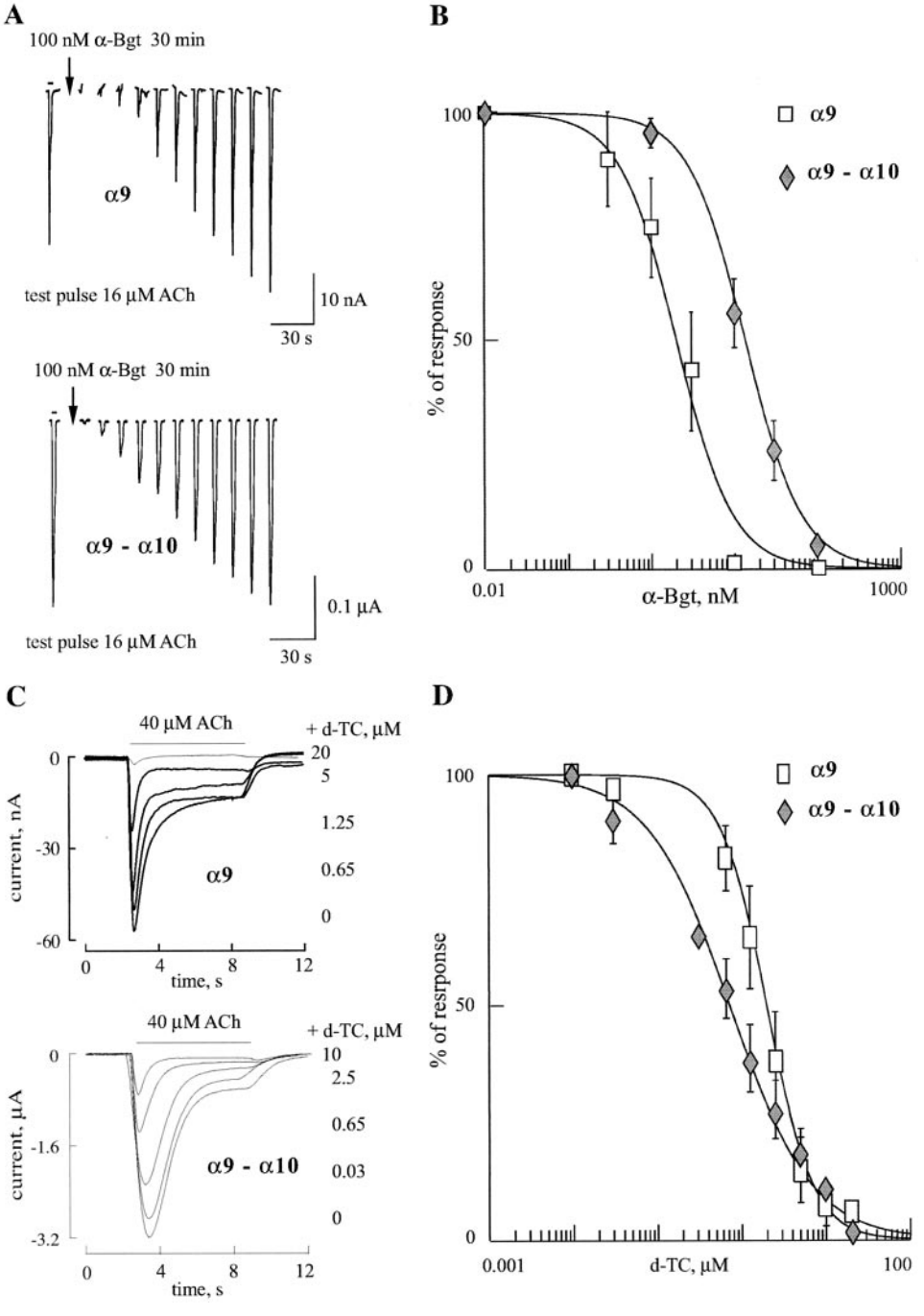

Fig. 5. Sensitivity of α9 and α9-α10 to nicotinic receptor antagonists, α-Bgt and *d*-tubocurarine. A, the α9 and α9-α10 acetylcholine-evoked currents are reversibly blocked by α-Bgt. Time course of the recoveries from blockade for two typical recordings are illustrated. B, concentration response inhibition relationship for α9 (squares) and α9-α10 (diamonds). Lines through the data points are the best fit obtained with a Hill equation with respective IC_{50} values of 2.1 and 14 nM and nH of 1.3 and 1.3 for α9 and α9-α10. C, effects of *d*-tubocurarine on the amplitude and time course of acetylcholine evoked currents. *d*-Tubocurarine was both pre- (20 s) and coapplied with a fixed concentration of acetylcholine (40 μM, 5 s). D, dose-response inhibition profile, measured at the peak current, for the α9 (squares) and α9-α10 (diamonds). Lines correspond to the best fits obtained with the Hill equation with respective IC_{50} values of 2 and 0.73 μM and nH of 1.6 and 0.9 for α9 and α9-α10 (n = 4).

TABLE 2
Determination of [^{125}I]α-Bgt binding to the surface of α9- or α9+α10-injected oocytes.
Values are indicated in femtomoles/oocyte with their respective standard error, with the number of cells tested in parenthesis.

	Non-Injected	α9-Injected	α9 + α10-Injected
^{125}I-α-Bgt binding (fmol/oocyte)	0.09 ± 0.04 (24)	1.08 ± 0.9 (16)	0.49 ± 0.32 (16)

response to acetylcholine in oocytes expressing the α9:α10-chimera with an average of 12.6 μA ± 1.5 (n = 12). The concentration-response relationship for acetylcholine further revealed an enhanced sensitivity of the chimera to this agonist accompanied by a higher Hill coefficient. On the basis of our current structure function relationship knowledge, it would be predicted that the chimera should display the ligand-binding properties of the α9-receptor and the ionic pore properties of α10-containing receptors. Determination of the concentration-response inhibition by *d*-tubocurarine illustrates that indeed the α9:α10-chimera displays a higher sensitivity than oocytes expressing the α9:α10-mixture (Fig. 7C). Moreover, the chimera sensitivity to α-bgt is closer to α9-homomeric than α10-containing receptors with a lower IC_{50} and faster recovery (Fig. 7D).

A high calcium permeability of acetylcholine receptors expressed at the outer hair cells has been shown to be one of the key features of the efferent control of the cochlea (Housley and Ashmore, 1992). We have examined the calcium permeability of the α9-α10-heteromer and α9:α10-chimera. In agreement with previous observation (Katz et al., 2000), reduction of the calcium concentration caused a significant increase of the ACh-evoked current of the three receptor subtypes (Fig. 8A) and a voltage-dependent blockade caused by calcium was also detected (not shown). When calcium was omitted from the extracellular medium a reduction of the responses was observed. As seen from data presented in Fig. 8, B and C, the three receptors each display a marked permeability to calcium.

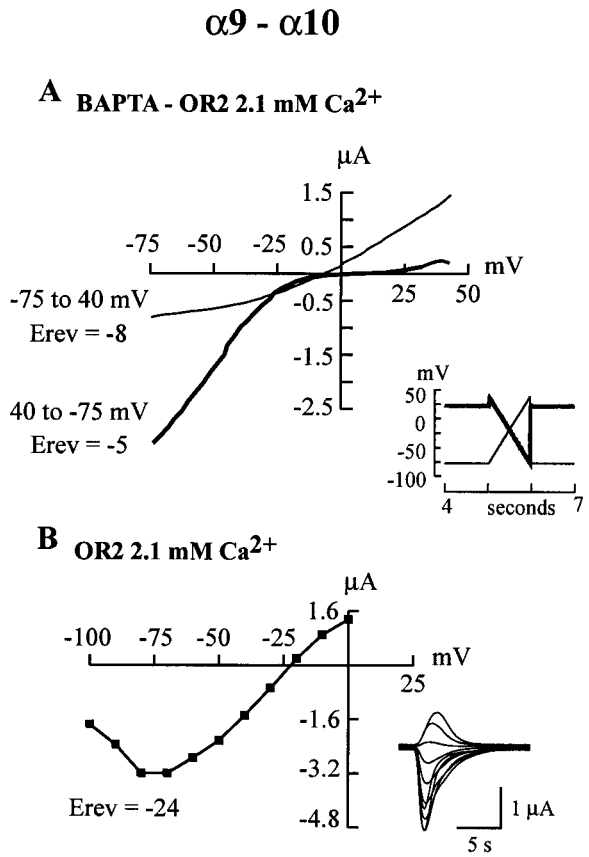

Fig. 6. Reversal potential of the ACh-evoked currents at α9-α10 receptors. A, current-voltage (I-V) was measured using a sawtooth voltage protocol (ranging from 40 to −75 mV, 1800 ms, thick trace) at the peak of the ACh-evoked current. Subtraction of the passive cell properties was obtained by repeating the same measure in absence of ACh. The thin line illustrates the I-V curve recorded in the same condition for a ramp starting at −75 mV and ending at +40 mV. To minimize chloride contamination, oocytes were incubated for at least 6 h in BAPTA-AM (100 μM). B, I-V relationship measured at steady holding potentials. To support the eye, data points have been connected by straight line. Inset, superposition of the current traces measured in B (ACh 1 mM, 3s).

Discussion

Although a fair number of genes coding for neuronal nAChRs have already been identified it is clear that reconstitution experiments have failed to describe all the subtypes observed in native cells (Pugh et al., 1995; Sorenson and Gallagher, 1996; Cuevas and Berg, 1998). The sequencing of the full genome of the nematode *Caenorhabditis elegans* has revealed the existence of over 40 potential genes encoding nicotinic acetylcholine receptor subunits in this organism (Littleton and Ganetzky, 2000), whereas to date only 16 nAChR subunits have been cloned in vertebrates (Lindstrom, 1997). Thus, yet undiscovered subunit could account for the existence of novel receptor proteins. In this work, we present evidence for the existence of a new nAChR subtype that would be composed by the association of α9 with a novel α10-subunit.

When expressed in *X. laevis* oocytes, the human α9-subunit was able to form recombinant homomeric channels activated by acetylcholine with properties similar to those reported for the rat α9 (Elgoyhen et al., 1994). As for the rat α9, the currents recorded were small (rarely over 100 nA), compared with those obtained with other nicotinic subunits that can form functional homomeric receptors, such as α7 or α8 (Couturier et al., 1990; Bertrand et al., 1993; Gerzanich et al., 1994; Gotti et al., 1994).

Despite its sequence homology with α9, the α10-subunit failed to reconstitute a functional receptor alone or in combination with other nAChR subunits. However, the coexpression of human α9- and α10-subunits resulted in a dramatic increase (about 100-fold) of the amplitude of the acetylcholine-evoked currents compared with that obtained with α9 alone. The binding experiments carried out with the ^{125}I-α-bgt on oocytes injected either with α9 alone or the mixture α9-α10 yielded surprising results. First, oocytes injected with α9 alone displayed a significant amount of α-bgt binding, whereas very small or no detectable currents could be measured in sibling oocytes. This suggests that α9-subunits are properly synthesized by the oocyte machinery and inserted in the plasma membrane where they form high-affinity α-Bgt binding sites. For some unknown reasons, however, these

proteins lack functionality. Second, coinjection of α9 and α10 yielded functional nAChRs and robust currents could be recorded without displaying a significant difference in α-bgt labeling than oocytes injected with α9 alone. These data illustrate that failure of α9-subunit to produce functional receptors must be attributed to the assembly and formation of an activatable receptor but not to the transport and insertion of α9 in the membrane. To challenge this hypothesis further we have compared the pharmacological profile of α9-expressing oocytes versus sibling cells injected with the α9-α10-mixture. Experiments carried out with antagonists such as α-bgt or *d*-tubocurarine revealed that addition of α10 significantly modified the α9 pharmacological profile. Because it is known that the ligand binding site resides at the interface between the α- and the adjacent subunit (Corringer et al., 1998; Sine et al., 1998), this result indicates that the α10-subunit must contribute to the formation of the agonist binding site.

The α9- and α10-subunits are clearly structurally related and display important differences with the other known nAChR α-subunits. The discovery that both subunits needed to be associated to form a functional receptor contrasts with the supposed homomeric assembly of α9. The only other example of functional heteromeric nAChR resulting from assembly of α-subunits is the α7-α8 found in chick retina (Gotti et al., 1994), although in this case both subunits are able to form a functional homomeric receptor. We thus sought to understand the structural features behind the impossibility for α10 to form a functional homomeric receptor and the poor functional expression of α9 alone by studying an α9:α10-chimera in which the extracellular domain of the α9-subunit was maintained, whereas all the rest of the pro-

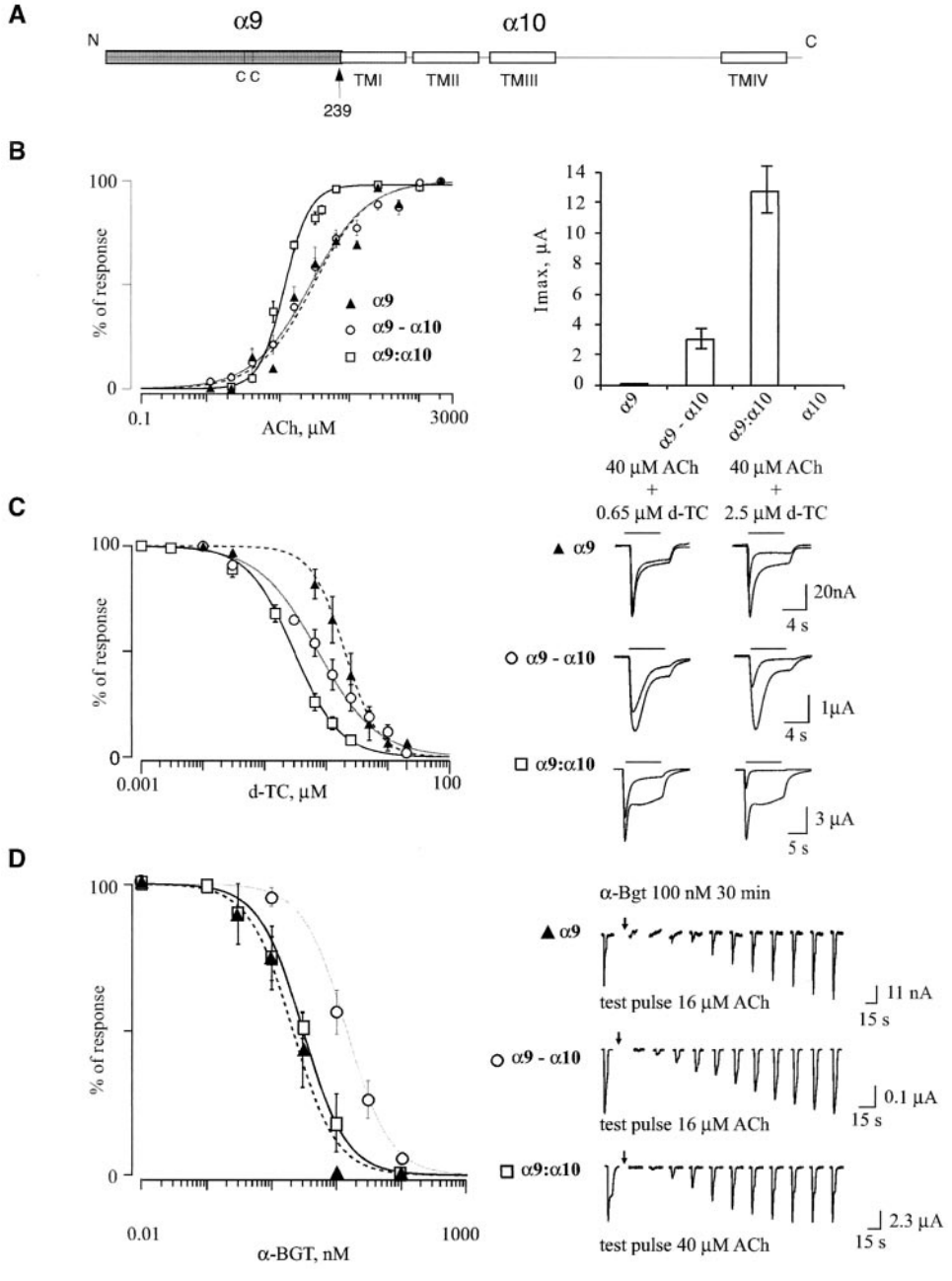

Fig. 7. The α9:α10-chimera reveals properties of the ligand binding site and the ionic pore. A, schematic representation of the α9:α10-chimera (dark area = α9-segment). The arrow indicates the point of fusion between the two proteins. B, acetylcholine sensitivity of the α9:α10-chimera is compared with those of oocytes expressing either α9- or α9-α10-receptors (left). Lines are the best fit obtained with the empirical Hill equation with an EC_{50} of 10 μM and *nH* of 1.5. Average currents evoked by saturating acetylcholine concentrations are represented for the different cDNA expression (right). Numbers of cells tested in each condition were, respectively, of 18 for α9, 29 for α9-α10, 12 for α9:α10, and 24 for α10. C, differential sensitivity of α9:α10 to *d*-tubocurarine. Lines through the data points are the best fits obtained with the empirical Hill equation an IC_{50} of 0.3 μM ± 0.04 and *nH* of and 1.16 (n = 7). Typical acetylcholine evoked currents recorded in control and presence of *d*-tubocurarine are shown in the right. D, concentration-response inhibition profile of α-Bgt reveals a higher sensitivity of the α9:α10-chimera. Best fit of the data points (continuous line) was obtained with the Hill equation with an IC_{50} of 3 nM and *nH* of 1.3. Typical recovery from blockade are represented by the successive acetylcholine evoked currents presented in the right.

tein was substituted by the α10-sequence. The very large acetylcholine-evoked currents recorded in oocytes injected with this α9:α10-chimera alone indicate that exchange of the α10 N-terminal domain was enough to restore its functionality. This finding can be interpreted either by the lack of homomerization of the unmodified α10-subunit or its incapacity to form a functional acetylcholine-binding site. In addition, these data illustrate that the ionic pore and gating properties are maintained in the α10-subunit.

The exchange of functional domain implies, as demonstrated with the serotoninergic receptor (Eiselé et al., 1993), that ligand-binding properties belong to the protein constituting the N-terminal domain, whereas the ionic pore characteristics are defined by the fusing protein segment. In agreement with this prediction, the difference between α9 and α10 for the competitive antagonist α-bgt was conserved in the chimera as similar to that of α9, whereas the blockade by *d*-TC was closer to that of α10-containing receptors suggesting again the heteromeric nature of α9-α10-receptors.

This α9-α10-receptor is a peculiar nicotinic receptor, both in terms of structure and functional property. One of the main issue is the functional significance of this novel nAChR. Efferent modulation of the cochlea OHCs is mediated by acetylcholine through a nicotinic receptor that exhibits a pharmacological profile resembling that described for α9- and α9-α10-receptors (Guth and Norris, 1996). Activation of this nAChR causes a transient influx of calcium that in turn activates hyperpolarizing calcium-dependent potassium channels (Blanchet et al., 1996). The pharmacology of α9-subunit reconstituted in oocytes (Elgoyhen et al., 1994) corresponds to that of native receptors expressed by vertebrate hair cells. Moreover, α9-null mice were shown to exhibit an absence of suppression of cochlear responses during efferent fiber activation (Vetter et al., 1999), thus demonstrating the role of α9-containing nAChR in the modulation of the cochlear response. The poor functional response of homomeric α9-receptor in oocyte suggests that additional subunit(s) might be required to obtain the calcium influx required to produce the activation of the calcium-dependent potassium conductance observed in vitro. Correctly processed α10-mRNA was found in the cochlea and we showed that the presence of α10-subunit together with α9 not only dramatically increased ACh-evoked currents but also preserved the receptor pharmacology similar to that observed in OHCs. In addition, affinity of α-bgt reported for isolated guinea pig OHCs (K_d = 62 nM; Lawoko et al., 1995) further illustrates a closer match to α9-α10 than α9 alone. This evidence supports the hypothesis that the α10-subunit must be contained in functional receptor complexes expressed by these sensory cells.

The coexpression of both subunits in the same region of the pituitary gland, the pars tuberalis, suggests another role for α9-α10-receptor. This region is in rat and in other mammals a major neuroendocrine target for melatonin, which regulates photoperiodical changes in prolactin secretion. Activation of pars tuberalis-specific cells is thought to trigger the release of a yet uncharacterized peptide, "tuberalin," which would in turn provoke the liberation of prolactin hormone from the pars distalis region (Morgan, 2000). Nicotinic receptors have been shown to modulate hormonal secretion in pituitary and adrenal gland (Gu et al., 1996; Matta et al., 1998). α9-α10-receptors could thus be involved in the control of a specific pars tuberalis endocrine system.

Recently, studies have suggested a role for α9-containing nAChRs in regulating keratinocyte adhesion (Grando, 1997). In particular, Nguyen et al. (2000) have shown that anti-α9

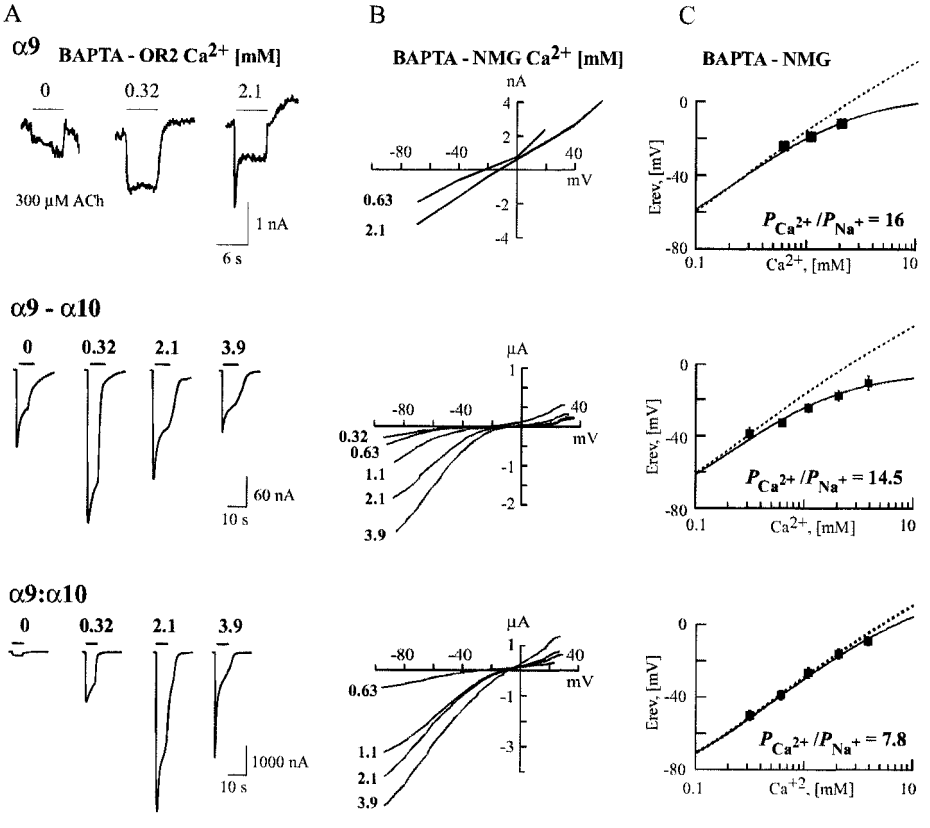

Fig. 8. Effects of extracellular calcium and calcium permeability of α9, α9-α10, and α9:α10 receptors. A, Typical ACh-evoked currents recorded in α9 (top traces), α9-α10 (middle traces), and α9: α10 (lower traces) expressing oocytes. Cells were held at −70 mV and challenged with 300 μM ACh (indicated by the bars) in different external calcium concentrations, values indicated above the traces. B, current voltage relationships recorded in different external calcium concentration in *N*-methyl-D-glucamine medium and BAPTA-AM. C, plot of the reversal potential, measured in C, as a function of the extracellular calcium concentration. Dashed lines indicate the best fit obtained with eq. 1, derived from the Goldman-Hodgkin-Katz equation with a *p*Na/*p*K of 0.65. Continuous lines were obtained using the same equation multiplied by an empirical Hill equation to take into account the calcium blockade. Relative calcium permeability for the three receptor types are indicated.

antibodies were present in the serum of patients affected by the autoimmune disease *Pemphigus vulgaris* and that the acantholysis resulting from this disease could be linked to a block of α9-containing receptors. Interestingly, this antibody effect could be reversed by the addition of carbachol, a cholinergic agonist that we have demonstrated to be active on α9-α10-receptors. We have shown that α10-subunit is also expressed in these cells and therefore that α9-α10-receptors are probably the functional nAChRs involved in the modulation of keratinocyte adhesion. The cholinergic pathway involved in this process is still unknown but the distinctive pharmacological profile of α9-α10-receptor suggests that specific agonists could have a therapeutic effect on such skin diseases.

The conclusion that α10-subunit is probably associated in vivo with α9 to form a novel subtype of nicotinic receptor involved in different physiological systems further illustrates the complexity of this receptor family. In a very recent publication, Elgoyhen et al. (2001) have reported the cloning and characterization of the rat α10-subunit. Similarly to the human α10, the rat α10 can assemble with α9 to form functional receptors and is expressed in cochlear hair cells. Whether α10 might be involved in the composition of other atypical nAChRs remains to be determined.

Acknowledgments

We thank Danielle Gaudeau and Monique Vasseur for excellent technical assistance, Sandrine Poea for scientific discussion and Guy Rebillard (INSERM U254, Montpellier) for the gift of RT reactions from rat cochlea. UB/OC-2 immortalized cochlear cells were kindly provided by Dr. M. Holley (Dept. of Physiology, University of Bristol, UK).

References

Anand R, Peng X, Balesta JJ, and Lindstrom J (1993) Pharmacological characterization of α-bungarotoxin-sensitive acetylcholine receptors immunoisolated from chick retina: contrasting properties of α7 and α8 subunit-containing subtypes. *Mol Pharmacol* **44:**1046–1050.

Bertrand D, Cooper E, Valera S, Rungger D, and Ballivet M (1991) Electrophysiology of neuronal nicotinic acetylcholine receptors expressed in *Xenopus* oocytes following nuclear injection of genes or cDNA, in *Methods in Neuroscience* (Conn M ed) vol 4, pp 174–193, Academic Press, New York.

Bertrand D, Galzi JL, Devillers-Thiéry A, Bertrand S, and Changeux JP (1993) Mutations at two distinct sites within the channel domain M2 alter calcium permeability of neuronal α7 nicotinic receptor. *Proc Natl Acad Sci USA* **90:**6971–6975.

Blanchet C, Erostegui C, Sugasawa M, and Dulon D (1996) Acetylcholine-induced potassium current of guinea pig outer cells: its dependence on a calcium influx through nicotinic-like receptors. *J Neurosci* **16:**2574–2584.

Boton R, Dascal N, Gillo B, and Lass Y (1989) Two calcium-activated chloride conductances in *Xenopus laevis* oocytes permeabilized with the ionophore A23187. *J Physiol* **408:**511–534.

Boyd RT (1997) The molecular biology of neuronal nicotinic acetylcholine receptors. *Crit Rev Tox* **27:**299–318.

Corringer PJ, Bertrand S, Bohler S, Edelstein SJ, Changeux JP, and Bertrand D (1998) Critical elements determining diversity in agonist binding and desensitization of neuronal nicotinic acetylcholine receptors. *J Neurosci* **18:**648–657.

Couturier S, Bertrand D, Matter JM, Hernandez MC, Bertrand S, Millar N, Valera S, Barkas T, and Ballivet M (1990) A neuronal nicotinic acetylcholine receptor subunit (α7) is developmentally regulated and forms a homomeric channel blocked by α-bungarotoxin. *Neuron* **5:**847–856.

Cuevas J and Berg DK (1998) Mammalian nicotinic receptors with α7 subunits that slowly desensitize and rapidly recover from α-bungarotoxin blockade. *J Neurosci* **18:**10335–10344.

Eiselé J, Bertrand S, Galzi JL, Devillers-Thiery A, Changeux JP, and Bertrand D (1993) Chimaeric nicotinic-serotoninergic receptor combines distinct ligand binding and channels specificities. *Nature (Lond)* **366:**479–483.

Elgoyhen AB, Johnson DS, Boulter J, Vetter DE, and Heinemann S (1994) Alpha 9: an acetylcholine receptor with novel pharmacological properties expressed in rat cochlear hair cells. *Cell* **79:**705–715.

Elgoyhen AB, Vetter DE, Katz E, Rothlin CV, Heinemann S, and Boulter J (2001) a10 A determinant of nicotinic cholinergic function in mammalian vestibular and cochlear mechanosensory hair cells. *Proc Natl Acad Sci USA* **98:**3501–3506.

Erostegui C, Norris CH, and Bobbin RP (1994) In vitro pharmacological characterization of a cholinergic receptor on outer hair cells. *Hear Res* **74:**135–147.

Freedman R, Adler LE, Bickford P, Byerley W, Coon H, Cullum CM, Griffith JM, Harris JG, Leonard S, Miller C, et al. (1994) Schizophrenia and nicotinic receptors. *Harvard Rev Psychiatry* **2:**179–192.

Galzi JL and Changeux JP (1995) Neuronal nicotinic receptors: molecular organization and regulations. *Neuropharmacology* **34:**563–582.

Gerzanich V, Anand R, and Lindstrom J (1994) Homomers of α8 subunits of nicotinic receptors functionally expressed in *Xenopus* oocytes exhibit similar channel but contrasting binding site properties compared to α7 homomers. *Mol Pharmacol* **45:**212–220.

Gotti C, Hanke W, Maury K, Moretti M, Ballivet M, Clementi F, and Bertrand D (1994) Pharmacology and biophysical properties of the alpha 7 and alpha 7-alpha 8 alpha-bungarotoxin receptors immunopurified from the chick optic lobe. *Eur J Neurosci* **6:**1281–1291.

Grando SA (1997) Biological functions of keratinocytes cholinergic receptors. *J Invest Dermatol Symp Proc* **2:**41–48.

Gu H, Wenger BW, Lopez I, McKay SB, Boyd RT, and McKay DB (1996) Characterization and localization of adrenal nicotinic acetylcholine receptors: evidence that mAb35-nicotinic receptors are the receptors mediating adrenal catecholamine secretion. *J Neurochem* **66:**1454–1461.

Guth PS and Norris CH (1996) The hair cell acetylcholine receptors: a synthesis. *Hear Res* **98:**1–8.

Housley GD and Ashmore JF (1992) Ionic currents of outer hair cells isolated from the guinea-pig cochlea. *J Physiol* **448:**73–98.

Jagger DJ, Griesenger CB, Rivolta MN, Holley MC, and Ashmore JF (2000) Calcium signalling mediated by the 9 acetylcholine receptor cochlear cell line from the immortomouse. *J Physiol* **527:**49–54.

Katz E, Verbitsky M, Rothlin CV, Vetter DE, Heinemann SF, and Elgoyhen AB (2000) High calcium permeability and calcium block of the alpha9 nicotinic acetylcholine receptor. *Hear Res* **141:**117–128.

Lawoko G, Jarlebark L, and Heilbronn E (1995) Ligand-binding properties of an unusual nicotinic acetylcholine receptor subtype on isolated outer hair cells from guinea pig cochlea. *Neurosci Lett* **195:**64–68.

Lindstrom J (1997) Nicotinic acetylcholine receptors in health and disease. *Mol Neurobiol* **15:**193–222.

Littleton JT and Ganetzky B (2000) Ion channels and synaptic organization: analysis of the *Drosophila* genome. *Neuron* **26:**35–43.

Mathie A, Colquhoun D, and Cull-Candy SG (1990) Rectification of currents activated by nicotinic acetylcholine receptors in rat sympathetic ganglion neurones. *J Physiol* **427:**625–655.

Matta SG, Fu Y, Valentine JD, and Sharp BM (1998) Response to the hypothalamo-pituitary-adrenal axis to nicotine. *Psychoneuroendocrinology* **23:**103–113.

Morgan PJ (2000) The pars tuberalis: the missing link in the photoperiodic regulation of prolactin secretion ? *J Neuroendocrinol* **12:**287–295.

Nguyen VT, Ndoye A, and Grando SA (2000) Novel human α9 acetylcholine receptor regulating keratinocyte adhesion is targeted by *Penphigus vulgaris* autoimmunity. *Am J Pathol* **157:**1377–1391.

Papke RL, Bencherif M, and Lippiello P (1996) An evaluation of neuronal nicotinic acetylcholine receptor activation by quaternary nitrogen compounds indicates that choline is selective for the alpha 7 subtype. *Neurosci Lett* **213:**201–204.

Puel JL (1995) Chemical synaptic transmission in the cochlea. *Prog Neurobiol* **47:**449–476.

Pugh PC, Corriveau RA, Conroy WG, and Berg DK (1995) Novel subpopulation of neuronal acetylcholine receptors among those binding α-bungarotoxin. *Mol Pharmacol* **47:**717–725.

Oliver D, Klöcker N, Schuck J, Baukrowitz T, Ruppersberg JP, and Fakler B (2000) Gating of Ca^{2+}-activated K^+ channels controls fast inhibitory synaptic transmission at auditory outer hair cells. *Neuron* **26:**595–601.

Sine SM, Bren N, and Quiram PA (1998) Molecular dissection of subunit interfaces in the nicotinic acetylcholine receptor. *J Physiol (Paris)* **92:**101–105.

Sorenson EM and Gallagher JP (1996) The membrane hyperpolarization of rat dorsolateral septal nucleus neurons is mediated by a novel nicotinic receptor. *J Pharmacol Exp Ther* **277:**1733–1743.

Vetter DE, Liberman MC, Mann J, Barhanin J, Boulter J, Brown MC, Saffiote-Kolman J, Heinemann SF, and Elgoyhen AB (1999) Role of α9 nicotinic ACh receptor subunits in the development and function of cochlear efferent innervation. *Neuron* **23:**93–103.

Address correspondence to: Frédéric Sgard, Department of Molecular and Functional Genomics, Sanofi-Synthélabo, 10 Rue des Carrières 92500 Rueil-Malmaison, France. E-mail: frederic.sgard@sanofi-synthelabo.com